Available online at www.sciencedirect.com
ScienceDirect
Trans. Nonferrous Met. Soc. China 27(2017) 1815−1821
Transactions of Nonferrous Metals Society of China
www.tnmsc.cn

Nanospike surface-modified bionic porous titanium implant and in vitro osteogenic performance

Guo-hui WANG[1] , Hua FU[1] , Ke-chao ZHOU[2], Yan-zhong ZHAO[1], Shai-hong ZHU[1]

1. Third Xiangya Hospital of Central South University, Central South University, Changsha 410013, China;
2. State Key Laboratory of Powder Metallurgy, Central South University, Changsha 410083, China

Received 4 May 2017; accepted 30 July 2017

Abstract: This work aimed to prepare the nanospike surface-modified bionic porous titanium implants that feature favorable osteointegration performance and anti-bacterial functions. The implant was prepared using freeze casting, and nanospike surface-modification of the implant was performed using thermal oxidation. The pore morphology and size, mechanical properties, and osteogenic performance of the implants were analyzed and discussed. The results showed that when the volume ratio of titanium powder in slurry was set to be 10%, the porosity, pore diameter, compressive strength, and elastic modulus of the porous samples were (58.32±1.08)%, (126.17±18.64) μm, (58.51±20.38) MPa and (1.70±0.52) GPa, respectively. When the porous sample was sintered at a temperature of 1200 °C for 1 h, these values were (58.24±1.50)%, (124.16±13.64) μm, (54.77±27.55) MPa and (1.63±0.30) GPa, respectively. The nanospike surface-modified bionic porous titanium implants had favorable pore morphology and size, mechanical properties and osteointegration performance through technology optimization, and showed significant clinical application prospect.

Key words: nanospike surface-modification; bionic porous titanium; osteogenic performance; freeze casting; thermal oxidation

1 Introduction

Since the elastic moduli of titanium and titanium alloy implants are higher than those of natural cortex bone [1], there is merely mechanical integration between the implants and bone rather than biological integration when it is implanted into a human body as a substitute material for bone. This, to some extent, has significantly increased risks of failure of bone transplantation, and is thus restricted in clinical application [2,3]. Porous metal materials serving as a new type of bone implants have become a key research topic in improving the osteointegration performance of implants [4,5]. Anisotropy and gradient distribution of porous metal materials by freeze casting were found much similar to those of natural human bone materials. Thus, it is highly possible to prepare bionic porous titanium implants that feature both favorable mechanical properties and similar pore morphology and sizes to human bone tissue through technology optimization [6−8].

Special responses and interactions between bionic bone implants with favorable osseointegration performance, as well as living bone tissue cells are required to form bio-integration by inducing osteoblasts to grow in the implant's porous structure. Compared with traditional porous materials, nanostructured porous implants are able to alter cell behavior on material surfaces by regulating the adsorption of macromolecules, e.g., proteins, as well as the cells' biological responses, thereby improving the adhesive and multiplication capacities of osteoblasts [9,10]. In previous research [11], an anti-bacterial nanospike was formed on the porous surface of titanium implants by applying a thermal oxidation method. And this structure showed effective performance in preventing bacteria from developing and multiplying on the implant surface, which can cause implant looseness, reoperation, and serious complications. Thus, this nanospike surface-modified structure showed significant clinical application value.

Foundation item: Projects (51290295, 51305464) supported by the National Natural Science Foundation of China; Project (2016JJ6156) supported by the Natural Science Foundation of Hunan Province, China; Project (2016JC2064) supported by the Key Research and Development Program of Hunan Province, China; Project (20130162120094) supported by the Specialized Research Fund for the Doctoral Program of Higher Education, China

Corresponding author: Shai-hong ZHU; Tel: +86-731-88618234; E-mail: zhushaihong@medmail.com.cn; Yan-zhong ZHAO; Tel: +86-731-88618669; E-mail: yanzhongzhao@163.com

DOI: 10.1016/S1003-6326(17)60204-8

However, further studies are needed to investigate the pore morphology and size, mechanical properties, and osteointegration performance of the nanospike surface-modified bionic porous titanium implants.

In the present work, the bionic porous titanium implant was prepared using freeze casting, and nanospikes modification of the surface was performed using a thermal oxidation method to obtain proper mechanical properties while ensuring porous structure and pore size, thereby improving osteointegration and physical antibacterial performance of the bionic implant.

2 Experimental

2.1 Preparation of porous titanium and nanospike surface-modification

Titanium powder with a particle size of <25 μm (Sigma-Aldrich, USA) and camphene (Fisher Scientific, UK), a solvent medium, were magnetically stirred in a water bath for 2 h at a temperature of 60 °C and a stirring rate of 800 r/min. Polyvinyl alcohol (PVA) was used as binder. The stirring vessel was covered to reduce solvent evaporation. The volume proportion of titanium powder in the slurry was 5%−20%. The mold was placed in the water bath case for precooling for 30 min at 20 °C, after which the prepared slurry was slowly poured into a precooled cylindrical mold with a thermally insulated top and bottom. After curing for 4 h, the mold was placed overnight in an environment at −20 °C for further cooling. Then, the samples were demolded and transferred to a vacuum freeze drying oven for sublimating for 24 h. The dried body was then put into the sintering furnace, where it was sintered firstly in vacuum at a heating rate of 1 °C/min until furnace temperature reached 400 °C, and then in argon atmosphere at a heating rate of 10 °C/min until furnace temperature reached 1200−1300 °C. Having been sintered for 1−4 h, the dried body was naturally cooled down to room temperature, and thereafter the porous titanium was prepared.

Samples were placed in the centre of a horizontal alumina tube furnace. After purging the tube with Ar, the temperature was increased to 850 °C at 15 °C/min. After reaching 850 °C, the Ar flow was diverted through a bubbler bottle containing acetone at 25 °C with the Ar flow rate of 300 mL/min. The temperature was kept at 850 °C for 45 min, after which the tube was allowed to cool under a flow of Ar at 500 mL/min. To remove the carbon from the as-synthesized nanospikes, the samples were heated to 600 °C at a rate of 10 °C /min.

2.2 Characterization and osteogenic performance

2.2.1 Samples cleaning and dimensional measurement

Sintered porous titanium specimens were cleaned in an ultrasonic cleaner for 15 min using analytically pure acetone (Fisher Scientific, UK), absolute ethyl alcohol (Fisher Scientific, UK), and double distilled water as cleaning agents. They then underwent drying in a high-temperature drying oven for 4 h at a temperature of 80 °C. An electronic analytical balance with an accuracy of 0.01 g was used to weigh the specimens. Finally, a Vernier caliper was used to measure 3 different positions of each specimen, and the mean value was then calculated. The accuracy was 0.01 cm.

2.2.2 Porous structures

The porous structures (porosity, degree of interconnection) of the porous Ti scaffolds and densifications of the Ti walls were characterized by scanning electron microscopy (FE-SEM, JSM−6330F, JEOL Techniques, Tokyo, Japan). The pore size was also analyzed from the SEM images of the samples prepared by infiltrating the porous Ti scaffolds with an epoxy resin.

2.2.3 Mechanical properties

The compressive strengths of the porous Ti scaffolds with a diameter and height of 16 and 20 mm, respectively, were examined using a screw-driven load frame at a crosshead speed of 5 mm/min. The stress and strain responses of the samples were monitored during the compressive strength tests. Five samples were tested to obtain the mean values and the standard deviation.

2.2.4 Adhesive function of MG63 osteosarcoma cells

The nano-modified titanium specimens, porous titanium specimens without nano-modification, and the control group of compact titanium specimens were kept in sealed preservation after sterilization and drying, and transferred and fixed to a 24-well cell culture plate. There were 3 specimens in each group. Then, 500 μL RPMI-1640 culture medium containing 10% fetal calf serum was added to each well on a clean bench. The culture solution was discarded after 24 h prewetting of specimens, and specimens were then gently cleaned twice using phosphate buffer solution (PBS). Digested MG63 osteosarcoma cells were diluted into a cell suspension with a density of 1×10^2 μL^{-1} per well, which was then dripped slowly from the specimen surface to the wells of the culture plate using a pipettor. Next, the culture plate was placed in an incubator containing 5% CO_2 for 8 h at a temperature of 37 °C and humidity of 95%.

The 24-well culture plate was taken out of the incubator on the fifth day. The culture solution was then discarded, and cells were cleaned gently 3 times using PBS buffer solution. The specimens were then transferred from the 24-well culture plate to empty containers, where they were fixed using 4 °C precooled glutaraldehyde with a volume fraction of 0.3% for 4 h. The specimens then underwent gradient dehydration for

10−15 min in 50%, 60%, 70%, 80%, 95% and 100% alcohol, tertiary butanol replacement for 1 min, critical point drying, and metal spraying, after which the distribution, adhesion, and growth of MG63 osteosarcoma cells on specimen surfaces were observed using SEM.

2.2.5 Detection of osteocalcin (OC) activity in human MG63 osteosarcoma cells

Cells were prepared in 24-well culture plates exactly as described in Section 2.2.4. Cells were assayed after 1, 3 and 5 d of incubation by discarding culture medium and gently rinsing with PBS twice, followed by adding 2.5 g/L trypsin to digest the cells for 2 min. Cell lysate (500 μL 0.2% TritonX-100) was added into each well to cover the cells, and then they were incubated overnight at 4 °C. An OC assay kit (ELASA method) was used to calculate the OC activity of the osteoblasts according to the manufacturer's instructions.

2.3 Statistical analysis

SPSS19.0 (SPSS Inc., Chicago, IL) software was used for statistical analysis. Experimental data are presented as means ± standard deviation ($\bar{x}$ ±S). Experimental data from two groups were compared using independent-sample Student's paired t tests. P<0.05 was considered statistically significant. ANOVA was used to test significant differences between multiple groups.

3 Results and discussion

3.1 Influence of Ti volume fraction in slurry on porous structure and mechanical properties of porous Ti

The specimen with a titanium volume fraction of 5% was found to be totally collapsed after sintering operation, with its original cylindrical shape basically destroyed. In comparison, specimens with 10%, 15%, and 20% volume fractions remained almost the same. Table 1 gives the shrinkage ratios of specimens. It could be inferred that specimen shrinkage rate declined with increasing volume fractions of titanium. As shown in the results, specimens with 10% and 20% volume fractions of titanium had the largest and smallest porosities, respectively. This is because the content of camphene that served as pore-forming material decreased progressively as the volume fraction of titanium increased, and the number of pores formed by the sublimation of pore-forming material after sintering also declined. Several studies [12,13] have indicated that the interconnecting pores in bone substitutes remained in the prerequisite conditions under which new bone developed and a porous structure with a porosity larger than 50% would provide bone growth in pores with an effective spatial environment. However, in this experiment, since the specimen with volume fraction of titanium of 20% had a porosity smaller than 50% after sintering, 20% was not a favorable volume fraction of titanium in the porous implant.

Table 1 Influence of volume fraction of titanium on properties of porous titanium specimens

φ(Ti)/%	Shrinkage ratio/%	Porosity/%	Aperture ratio/%
10	12.15	58.32±1.08	97.70
15	11.27	53.22±2.11	95.54
20	10.53	45.03±1.23	90.50

Under SEM, the morphology of porous titanium was radially distributed and concentrated in the middle of the cylinder (Fig. 1). When the slurry at 60 °C was poured into the cylindrical mold at 20 °C, a temperature gradient would be formed in the slurry between the periphery and center of the mold. The crystals in the slurry would grow from the periphery of the mold to the center in a radial pattern. After the camphene was sublimated, the outside-in radial morphology was formed in the implants. Specimens with different volume

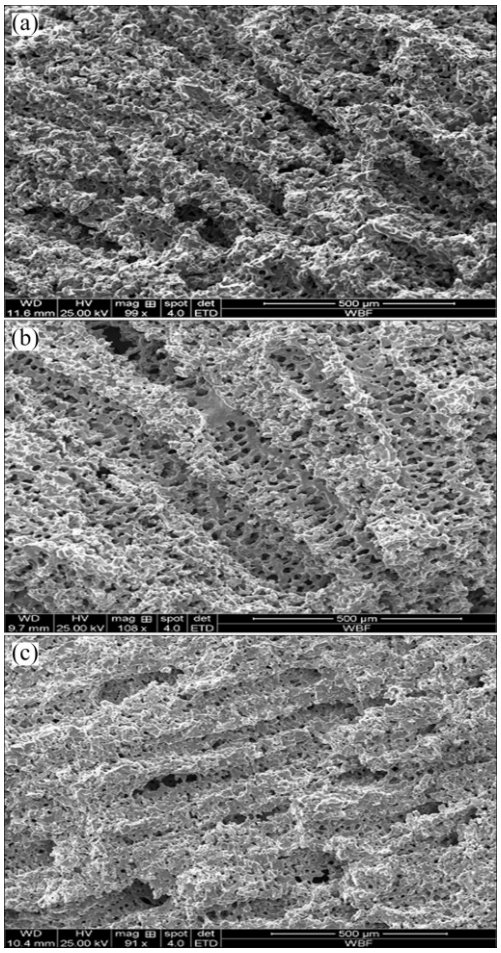

Fig. 1 SEM images of porous titanium with different titanium volume fractions in slurry: (a) 10%; (b) 15%; (c) 20%

fractions of titanium had varied pore diameters. Specifically, pore diameters of specimens with 10%, 15%, and 20% volume fractions of titanium were (126.17±18.64), (104.52±21.33) and (85.12±18.64) μm, respectively, indicating that the volume fraction of titanium had an effect on pore size. Pore diameter and pore connectivity of the sintered specimens decreased continuously as volume fraction increased. Of all factors affecting osseointegration between the porous implant and bone ingrowth in it, pore diameter is one of the major factors. According to previous studies [14,15], the pore diameter ranging from 100 to 400 μm was suitable for ingrowth of osteoblasts because it could provide this with appropriate pressure and tension by acting on cells' mechanoreceptors. Micro-pores larger than 100 μm met demands of inoculated cells for attachment, spreading, and multiplication, whereas micro-pores smaller than 100 μm could play an important role in cell metabolism and switching. As a result, pore diameters and connectivity of specimens with volume fractions of 10% and 15% were best suited for bone tissue ingrowth among all three groups of specimens.

Table 2 gives the compressive strength and elastic modulus of porous titanium specimens with different volume fractions of titanium. Compressive strength increased with rising volume fractions of titanium. The compressive strength was (58.51±20.38) and (250.03±41.23) MPa when volume fractions of titanium were 10% and 20%, respectively. Elastic modulus also increased from (1.70±0.52) to (5.50±0.22) GPa when the volume fraction of titanium increased from 10% to 20%. This suggested that mechanical properties of porous titanium specimens were affected by the volume fraction of titanium powder in the slurry: a higher volume fraction of titanium powder indicated a smaller proportion of camphene that served as a pore-forming agent in the slurry, which led to a low specimen porosity after sintering; moreover, the specimen whose volume fraction of titanium was 20% had the smallest porosity, most compact structure, and largest compressive strength and elastic modulus. Compressive strength of specimens in all three groups was higher than that of the human bone tissue, i.e., 10−60 MPa; meanwhile, the average elastic modulus was close to that of human bone tissue, i.e., 0.1−30 GPa. As a result, specimens in all three groups meet clinical requirements for bone implants.

Table 2 Influence of volume fraction of titanium on mechanical properties of porous titanium

φ(Ti)/%	Compressive strength/MPa	Elastic modulus/GPa
10	58.51±20.38	1.70±0.52
15	143.46±35.61	3.54±0.15
20	250.03±41.23	5.50±0.22

3.2 Influence of sintering temperature on porous structure and mechanical properties of porous Ti

Table 3 gives the results of specimen porosities at different sintering temperatures. Specimen porosity was the largest, i.e., (58.24±1.50)%, when the specimen was sintered at 1200 °C for 1 h, and this number declined to (45.99±2.15)% when the specimen was sintered at 1300 °C for 1 h, indicating that specimen porosity declined after sintering, while the shrinkage ratio (i.e., deformation heightened before and after sintering) increased and the aperture ratio decreased as sintering temperature increased. This was because the micro-pores between titanium powder particles on the pore wall integrated with each other or disappeared as sintering temperature and time increased, which led to pore−wall compaction of porous material, and closed channels that interconnected with each other via micro-pores, and thus, the porosity and aperture ratio declined after sintering.

Table 3 Influence of sintering temperature on properties of porous titanium specimens

Sintering temperature/°C	Shrinkage ratio/%	Porosity/ %	Aperture ratio/%
1200 (Sintering for 1 h)	12.59	58.24±1.50	97.30
1200 (Sintering for 4 h)	13.29	54.19±2.01	94.49
1300 (Sintering for 4 h)	15.55	45.99±2.15	92.50

Pore morphologies of porous titanium formed at different sintering temperatures were observed using SEM (Fig. 2). When sintering temperature was 1200 °C, diameters of smaller micro-pores between titanium powder particles on the pore wall of porous titanium were observed to decrease, and as sintering time increased, the sintering neck turned thicker. This suggested that titanium powder particles showed a higher degree of fusion as sintering temperature increased. The pore diameter decreased from (124.16±13.64) to (94.16±16.05) μm. Furthermore, the pore wall turned more compact when sintering temperature increased to 1300 °C because most micro-pores between titanium powder particles on the pore wall disappeared at this temperature. Finally, pore diameter declined to (90.35±2.01) μm after sintering. Thus, as sintering temperature increased, micro-pores between titanium powder particles on the pore wall integrated each other or disappeared, titanium powder particles showed a higher degree of fusion, and the pore wall was continuously compacted, which finally resulted in smaller pore diameters after sintering.

Table 4 gives the results of the mechanical properties test. Compressive strength and elastic modulus of sintered porous titanium specimens increased as

sintering temperature increased. Additionally, the pore wall turned more compact due to fusion between titanium powder particles. As a result, the compressive strength and elastic modulus of porous titanium specimens were increased.

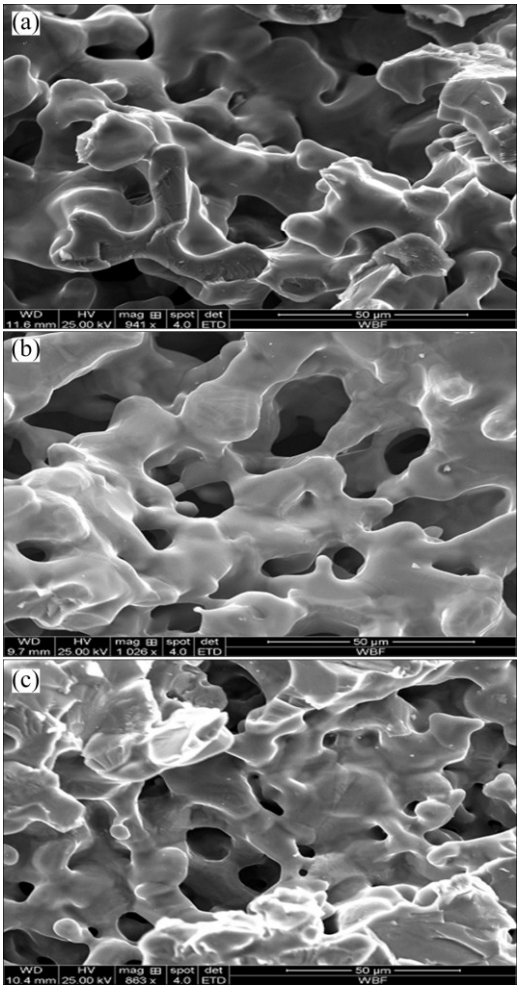

Fig. 2 SEM images of porous titanium specimen at different sintering temperatures: (a) 1200 °C (Sintered for 1 h); (b) 1200 °C (Sintered for 4 h); (c) 1300 °C (Sintered for 1 h)

Table 4 Influence of sintering temperature on mechanical properties of porous titanium

Sintering temperature/°C	Compressive strength/MPa	Elastic modulus/GPa
1200 (Sintered for 1 h)	54.77±27.55	1.63±0.30
1200 (Sintered for 4 h)	113.37±25.18	2.85±0.25
1300 (Sintered for 1 h)	147.12±15.53	2.99±0.12

3.3 Pore morphology after surface modification

As shown in Fig. 3, nanospikes were evenly distributed on the pore wall surface after thermal oxidation treatment. The size of the nanospikes developed on the substrate of the pore wall was about 200 nm.

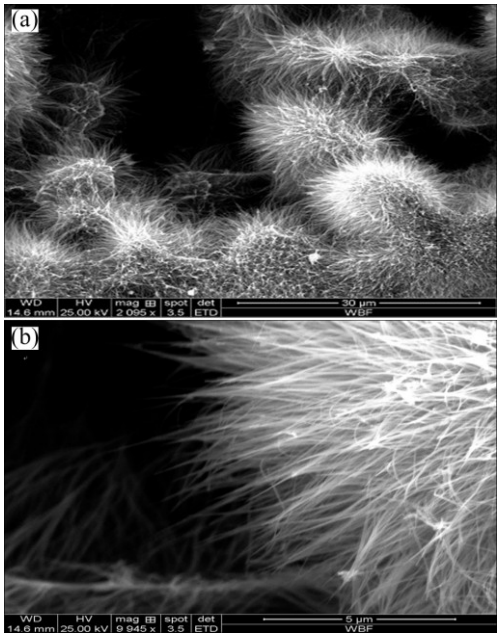

Fig. 3 SEM images of nanospike surface-modified porous titanium sample: (a) Low magnification; (b) High magnification

3.4 Adhesive function of MG63 osteosarcoma cells

Figure 4 shows the morphologic observation results of osteoblasts on the fifth day of attached growth on specimen surfaces. SEM observation suggested that MG63 osteosarcoma cells were spheroidal with fewer pseudopodia, and had insufficient spreading on the surface of compact titanium in the control group. However, they spread favorably on substrates of titanium materials in both nano-modified and unmodified groups. This was especially true for the material surface of the nano-modified group, where cell processes were attached to the material surface, the edge of pores, or within pores, and showed a tendency of migration into them. Furthermore, the cells with rich cytoplasm and pseudopodium structures spread polygonally or spindly. Some tiny synaptic structures reflecting the active state of cell growth could be observed at the ends of cell processes. Additionally, the porous structure and needle-like nanostructured surface modification promoted osteoblasts to be attached to materials, which might be attributed to the increase in interactions between osteoblasts and the substrate of the pore wall due to nanofiber structures on the material surface in the treated group, which made it easier for the attachment, growth, and multiplication of osteoblasts [16−18].

3.5 Detection of osteocalcin (OC) activity in human MG63 osteosarcoma cells

The OC activities of MG63 osteosarcoma cells were measured in different groups and it was found (Table 5) that the prolonged co-culture with different specimens

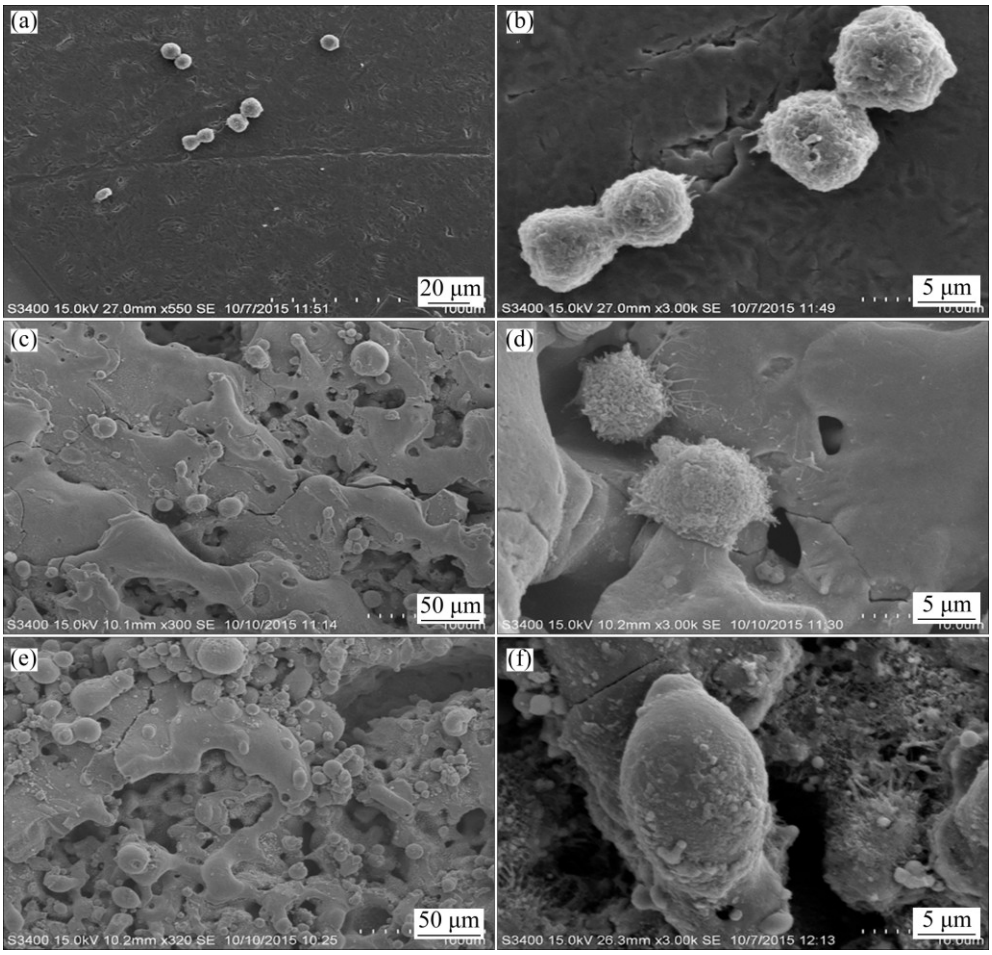

Fig. 4 SEM images of attachment and growth of osteoblasts on different specimen surfaces: (a, b) Control group; (c, d) Experimental group without nano-modification; (e, f) Experimental group with nano-modification

continually increased the OC activities of the cells. OC activities of osteoblasts co-cultured for 1 d with porous titanium in both experimental groups were not significantly higher than those in the dense titanium implant control group (P>0.05). No significant difference in OC activities was found between the two groups were significantly higher than those in the control group (P<0.05); in addition, OC activity in the modified experimental groups. OC activities for cells co-cultured for 3 and 5 d with porous titanium in both experimental group was significantly higher than that in the unmodified group (P<0.05). These results suggested that the porous structure and tertiary nanostructure of the pore gaps affected the OC activities of osteoblasts, as prolonged co-culture with nano-modified porous titanium showed the most enhanced OC activity.

Table 5 OC activity measured at different time after co-culturing of cells with different implant materials

Sample	n	OC activity/(μg·L^{-1})		
		Day 1	Day 3	Day 5
Modified experimental group	9	0.617±0.085	1.207±0.170*$^{\triangle}$	2.124±0.065*$^{\triangle}$
Unmodified experimental group	9	0.609±0.107	1.142±0.038*	2.007±0.168*
Control group	9	0.604±0.050	0.884±0.094	1.206±0.094

*P<0.05 compared with control group; $^{\triangle}P$<0.05 compared with unmodified experimental group

4 Conclusions

1) When the volume ratio of titanium powder in slurry was set to be 10% and the porous sample was sintered at a temperature of 1200 °C for 1 h, the bionic porous titanium implants that feature favorable pore morphology and size, mechanical properties through technology optimization showed significant clinical application prospect.

2) Nanospike structure was evenly distributed on the substrate of the pore wall after thermal oxidation treatment, and the size of the nanospikes was about 200 nm.

3) The nanospike surface-modified bionic porous titanium implants had favorable osteointegration performance.

Acknowledgements

The authors would like to thank Professor Su Bo in School of Oral and Dental Sciences, University of Bristol, UK for carring out nanospike surface-modification test.

References

[1] PULEO D A, NANCI A. Understanding and controlling the bone-implant interface [J]. Biomaterials, 1999, 20: 2311−2321.

[2] WANG Xiao-jian, XU Shan-qing, ZHOU Shi-wei, XU Wei, LEARY M, CHOONG P, QIAN M, BRANDT M, XIE Yi-min. Topological design and additive manufacturing of porous metals for bone scaffolds and orthopaedic implants: A review [J]. Biomaterials, 2016, 83: 127−141.

[3] RYAN G E, PANDIT A S, APATSIDIS D P. Porous titanium scaffolds fabricated using a rapid prototyping and powder metallurgy technique [J]. Biomaterials, 2008, 29: 3625−3635.

[4] LEVINE B. A new era in porous metals: Applications in orthopaedics [J]. Advanced Engineering Materials, 2008, 10: 788−792.

[5] QIN Jun-hua, CHEN Qing, YANG Chun-yuan, HUANG Yong. Research process on property and application of metal porous materials [J]. Journal of Alloys and Compounds, 2016, 654: 39−44.

[6] ULRIKE G K W, SCHECTER M, DONIUS A E, HUNGER P M. Biomaterials by freeze casting [J]. Phil Trans R Soc, 2010, 368: 2099−2121.

[7] SYLNAIN D. Freeze-casting of porous biomaterials: Structure, properties and opportunities [J]. Materials, 2010, 3: 1913−1927.

[8] PORTER M M, MCKITTRICK J, MEYERS M A. Biomimetic materials by freeze casting [J]. JOM, 2013, 65: 720−727.

[9] ZHAO Ling-zhou, WEI Yan-ping, Li Jian-xue, HAN Yong, YE Rui-dong, ZHANG Yu-mei. Initial osteoblast functions on Ti−5Zr−3Sn−5Mo−15Nb titanium alloy surfaces modified by microarc oxidation [J]. J Biomed Mater Res A, 2010, 92: 432−440.

[10] DINAN B, GALLEGO P D, LEE H, HANSFORD D, AKBAR S A. Thermally grown TiO_2 nanowires to improve cell growth and proliferation on titanium based materials[J]. Ceram Int, 2013, 39: 5949−5954.

[11] TERJS S, ANGELA H N, BO S. Bactericidal nanospike surfaces via thermal oxidation of Ti alloy substrates [J]. Materials Letters, 2016, 167: 22−26.

[12] de VASCONCELLOS L M R, OLIVEIRA F N, LEITE D D, de VASCONCELLOS L G O, do PRADO R F, RAMOS C J, GRACA M L A, CAIRO C A A, CARVALHO Y R. Novel production method of porous surface Ti samples for biomedical application [J]. J Mater Sci Mater Med, 2012, 23: 357−64.

[13] ZHANG Lei, RONAN L C B, CHALOTTE B, TERJE S, SU Bo. Gelatin freeze casting of biomimetic titanium alloy with anisotropic and gradient pore structure [J]. Biomed Mater, 2017, 12: 1−6.

[14] NUGROHO A W, LEADBEATER G, DAVIES I J. Processing of a porous titanium alloy from elemental powders using a solid state isothermal foaming technique [J]. J Mater Sci Mater Med, 2010, 21: 3103−3107.

[15] de VASCONCELLOS L M, LEITE D D, NASCIMENTO F O, de VASCONCELLOS L G, GRACA M L, CARVALHO Y R, CAIRO C A. Porous titanium for biomedical applications: An experimental study on rabbits [J]. Med Oral Patol Oral Cir Bucal, 2010, 15: 407−412.

[16] ROSS A M, JIANG Z X, BASTMEYER M, LAHANN J. Physical aspects of cell culture substrates: Topography, roughness, and elasticity [J]. Small, 2012, 8: 336−55.

[17] ROSALES-LEAL J I, RODRIGUZ-VALVERDE M A, MAZZAGLIA G, RAMÓN-TORREGROSA P J, DÍAZ-RODRÍGUEZ L, GARCIA-MARTINEZ O, VALLECILLO-CAPILLA M, RUIZ C, CABREIZO-VÍLCHEZ M A. Effect of roughness, wettability and morphology of engineered titanium surfaces on osteoblast-like cell adhesion [J]. Colloid Surface A, 2010, 365: 222−229.

[18] GITTENS R A, MCLACHLAN T, OLIVARES-NAVARRETE R, YE Cai, BERNER S, TANNENBAUM R, SCHWARTZ Z, SANDHAGE K H, BOYAN B D. The effects of combined micron-/submicron-scale surface roughness and nanoscale features on cell proliferation and differentiation [J]. Biomaterials, 2011, 32: 3395−3403.

纳米针状表面改性的仿生多孔钛植入体及体外成骨性能

王国慧[1]，付 华[1]，周科朝[2]，赵颜忠[1]，朱晒红[1]

1. 中南大学 湘雅三医院，长沙 410013；2. 中南大学 粉末冶金国家重点实验室，长沙 410083

摘 要：通过冷冻铸造和热氧化法制备一种新型兼具抗菌功能和良好骨整合性能的纳米针状表面改性仿生多孔钛植入体。分析和表征仿生多孔钛植入体的孔隙形貌和尺寸、力学性能和体外成骨性能。结果表明：当控制冷冻铸造工艺中浆料中钛粉体积比为 10%时，多孔试样的孔隙度为(58.32±1.08)%、孔径为(126.17±18.64) μm、压缩强度为(58.51±20.38) MPa、弹性模量为(1.70±0.52) GPa。在 1200 °C 烧结 1 h，多孔试样的孔隙度为(58.24±1.50)%、孔径为(124.16±13.64) μm、压缩强度为(54.77±27.55) MPa、弹性模量为(1.63±0.30) GPa。通过热氧化方法在多孔钛植入体试样的孔隙表面制备出均匀分布的纳米针状结构。通过对工艺的优化，制备出具有良好孔隙形貌和尺寸，同时具备良好力学性能和体外成骨性能的纳米针状表面改性仿生多孔钛植入体，具有重要的临床应用前景。

关键词：纳米针状表面改性；仿生多孔钛；成骨性能；冷冻铸造；热氧化法

(Edited by Sai-qian YUAN)